Bioorganic Chemistry 105 (2020) 104436

Contents lists available at ScienceDirect

Bioorganic Chemistry

journal homepage: www.elsevier.com/locate/bioorg

Hydroxamic acid with benzenesulfonamide: An effective scaffold for the development of broad-spectrum metallo-β-lactamase inhibitors

Jia-Qi Li, Cheng Chen, Min Yao, Le-Yun Sun, Han Gao, Jiazhu Chigan, Ke-Wu Yang *

Key Laboratory of Synthetic and Natural Functional Molecule of the Ministry of Education, College of Chemistry and Materials Science, Northwest University, Xi'an 710127, PR China

ARTICLE INFO

Keywords:
Antibiotic resistance
Metallo-β-lactamases
Inhibitor
Benzenesulfonamide
Hydroxamic acid

ABSTRACT

Given that β-lactam antibiotic resistance mediated by metallo-β-lactamases (MβLs) seriously threatens human health, we designed and synthesized nineteen hydroxamic acids with benzenesulfonamide, which exhibited broad-spectrum inhibition against four tested MβLs ImiS, L1, VIM-2 and IMP-1 (except **6**, **13** and **18** on IMP-1, and **18** on VIM-2), with an IC_{50} value in the range of 0.6–9.4, 1.3–27.4, 5.4–43.7 and 5.2–49.7 μM, respectively, and restored antibacterial activity of both cefazolin and meropenem, resulting in a 2–32-fold reduction in MIC of the antibiotics. Compound **17** shows reversible competitive inhibition on L1 with a K_i value of 2.5 μM and significantly reduced the bacterial load in the spleen and liver of mice infected by *E. coli* expressing L1. The docking studies suggest that **17** tightly binds to the Zn(II) of VIM-2 and CphA by the oxygen atoms of sulfonamide group, but coordinates with the Zn(II) of L1 through the oxygen atoms of hydroxamic acid group. These studies reveal that the hydroxamic acids with benzenesulfonamide are the potent scaffolds for the development of MβL inhibitors.

1. Introduction

Since people discovered penicillin in the 1920s and used it to fight bacteria [1], the β-lactam antibiotics have been developed as one of the most commonly and extremely important clinical antibacterial drugs for the treatment of bacterial infections [2]. However, the overuse of these antibiotics has exacerbated the production of resistant bacteria, which has become a critical public health threat [3]. Bacteria resistant to antibiotics in several ways, and the most common way is that bacteria hydrolyze antibiotics by the production of β-lactamases, which catalyze the cleavage of β-lactam rings of the antibiotics [2,4]. Due to differences in amino acid sequence homology, these enzymes have been categorized into classes A–D [5]. Class A, C and D enzymes are called serine β-lactamases (SβLs). These enzymes use a catalytic mechanism in which the active site of serine residue nucleophilically attacks the β-lactam carbonyl group, causing the β-lactam ring fracture. Class B enzymes, also called as metallo-β-lactamases (MβLs), are Zn(II)-dependent and utilize Zn(II) ions to catalyze the hydrolysis of the β-lactam ring. Based on amino acid sequence homology, MβLs are further divided into subclasses B1, B2 and B3 [6,7].

SβLs utilize an active-site serine inactivating the β-lactams in covalent mechanisms which can be targeted by β-lactamase inhibitors. So far, some SβL inhibitors are clinically available to overcome bacterial resistance through the combination with β-lactam antibiotics, such as clavulanic acid, sulbactam, tazobactam and avibactam [8,9], but there is no MβL inhibitor available [3]. To prevent the hydrolysis of β-lactam antibiotics by MβLs, a number of classes of MβL inhibitors have been reported, such as β-lactam analogues [10], thiols [11,12], carboxylic acids [13,14], ebselen [15], rhodanines [16], cyclic boronates [17] and others [18–21]. However, only few reports are on broad-spectrum inhibitors of MβLs. The broad-spectrum MβL inhibitor is the compound that inhibits several MβLs, even MβLs from several subclasses.

Hydroxamic acids have been extensively studied to matrix metalloproteinase targets, when combined with Zn(II) ions in the active centers of these enzymes, causing the enzyme to lose its catalytic activity [22]. For example, hydroxamic acid (SAHA, vorinostat; Fig. 1A), inhibit class I and II histone deacetylases (HDACs) by chelating Zn(II) ions at the active site and SAHA has been approved by Food and Drug Administration (FDA) for the treatment of *T*-cell lymphoma [23,24]. Hydroxamic acids have also been studied for inhibition of some MβLs [25,26]. Recently, we reported that the benzenesulfonamide exhibits strong enzymatic inhibition activity against ImiS [27]. This enlightened us to

* Corresponding author.
E-mail address: kwyang@nwu.edu.cn (K.-W. Yang).

https://doi.org/10.1016/j.bioorg.2020.104436
Received 29 June 2020; Received in revised form 10 September 2020; Accepted 26 October 2020
Available online 29 October 2020

cross linking the hydroxamic acid and sulfonamide group to develop MβLs inhibitors. Our goal is to develop broad-spectrum MβL inhibitor and use it in combination with β-lactam antibiotics to fight resistant bacterial infections.

Towards this goal, nineteen hydroxamic acids with benzenesulfonamides **1**–**18** and DSN (shown in Fig. 1) were designed, synthesized, characterized by ^{1}H and ^{13}C NMR and confirmed by HRMS (see Supporting Information). Inhibitory activity of the hydroxamic acids was evaluated with four MβLs from three subgroups of B1 (VIM-2 and IMP-1), B2 (ImiS) and B3 (L1), and the inhibitory mode was investigated. The antibacterial activity of antibiotics in combination with the inhibitors against drug-resistant bacteria was assayed *in vitro* (MIC) and *in vivo* (mice experiments). Also, the interaction of hydroxamic acids with the target enzymes was studied by molecular docking.

2. Results and discussion

2.1. Synthesis of hydroxamic acid

The hydroxamic acids with benzenesulfonamides **1**–**18** and DSN were synthesized based on two strategies: first, adjust the position (*o-*, *m-*, *p-*) of phenylsulfonamide relative to *N*-hydroxybenzamide, to define the optimal position where hydroxamic acids bind the active site of MβLs, which confers the best inhibitory effect; and second, adjust different substituent groups on *p*-position of phenylsulfonamide to test the effect on hydroxamic acid inhibitory activity. The hydroxamic acids were synthesized by previously reported methods [28,29]. Briefly, aminobenzoic acids reacted with benzenesulfonyl chlorides in K_2CO_3 aqueous solution, and the resulting mixture was acidified with HCl to give the benzenesulfonamide benzoic acids [28]. In the presence of the *N, N*-carbonyldiimidazole (CDI), the benzoic acids reacted with hydroxylamine hydrochloride for 24 h to afford the desired hydroxamic acids with benzenesulfonamides [29].

2.2. Activity evaluation of hydroxamic acids

To test if these hydroxamic acids were broad-spectrum inhibitors of MβLs, we selected VIM-2, IMP-1, ImiS and L1 as the representatives of MβLs for the test. The antibiotics were selected to be meropenem (for ImiS, monitoring at 300 nm) and cefazolin (for VIM-2, IMP-1 and L1, monitoring at 265 nm) as substrates. The concentration of substrate was 40 μM, and the concentrations of inhibitor were in the range of 0–20 μM, respectively [30–32]. All experimental data were obtained by the Agilent UV8453 spectrometer.

The synthetic compounds **1**–**18** were divided into three categories (Fig. 1), **1–8** *m*-substituted with 3-phenylsulfonamido, **9**–**13** *o*-substituted with 2-phenylsulfonamido, and **14**–**18** *p*-substituted with 4-phenylsulfonamido. Percent inhibition showed in Fig. S1 indicated that the hydroxamic acids synthesized exhibited 63–98% inhibition against ImiS, **14**–**18** exhibited >70% inhibitory activity on L1, and **17** showed broad-spectrum inhibition on VIM-2, IMP-1, ImiS and L1, with an inhibition rate >70%.

Hydroxamic acids concentrations causing 50% decrease in enzyme activity (IC_{50}) were determined. As shown in Table 1, the hydroxamic acids exhibited broad-spectrum inhibition against four tested MβLs ImiS, L1, VIM-2 and IMP-1 (except **6**, **13** and **18** on IMP-1, and **18** on VIM-2), with an IC_{50} value in the range of 0.6–9.4, 1.3–27.4, 5.4–43.7 and 5.2–49.7 μM, respectively. Also, the *m*- and *p*-substituted hydroxamic acids had better inhibitory activities against VIM-2 and L1, respectively, than the other substituted categories, and **17** was found to be the most potent inhibitor, with an IC_{50} value in the range of 1.3–9.9 μM, which is similar to the data (IC_{50} = 0.11–9.3 μM) of the benzenesulfonamide derivatives against ImiS [27]. In addition, for L1, **17** exhibited better inhibitory activity (IC_{50} = 1.3 μM) than **12** (IC_{50} = 7.8 μM), and then than **4** (IC_{50} = 12.7 μM). The analysis of the structure–activity relationship revealed that the *m*- and *p*-substituted sulfonyl group improved the inhibitory activity of the hydroxamic acids against VIM-2 and L1, respectively.

Given the broad-spectrum potency of hydroxamic acids against MβLs, the residual activities of four MβLs in the presence of inhibitor **17** at different concentrations were assayed, the generated inhibition curves (Fig. 2) shown that the inhibitor exhibited >80% inhibition (>20% residual activity) against VIM-2, IMP-1, ImiS and L1 at a concentration of 10, 40, 80 and 5 μM, respectively.

2.3. Inhibition mode of hydroxamic acids

Next, compound **17** was selected to determine K_i value and to

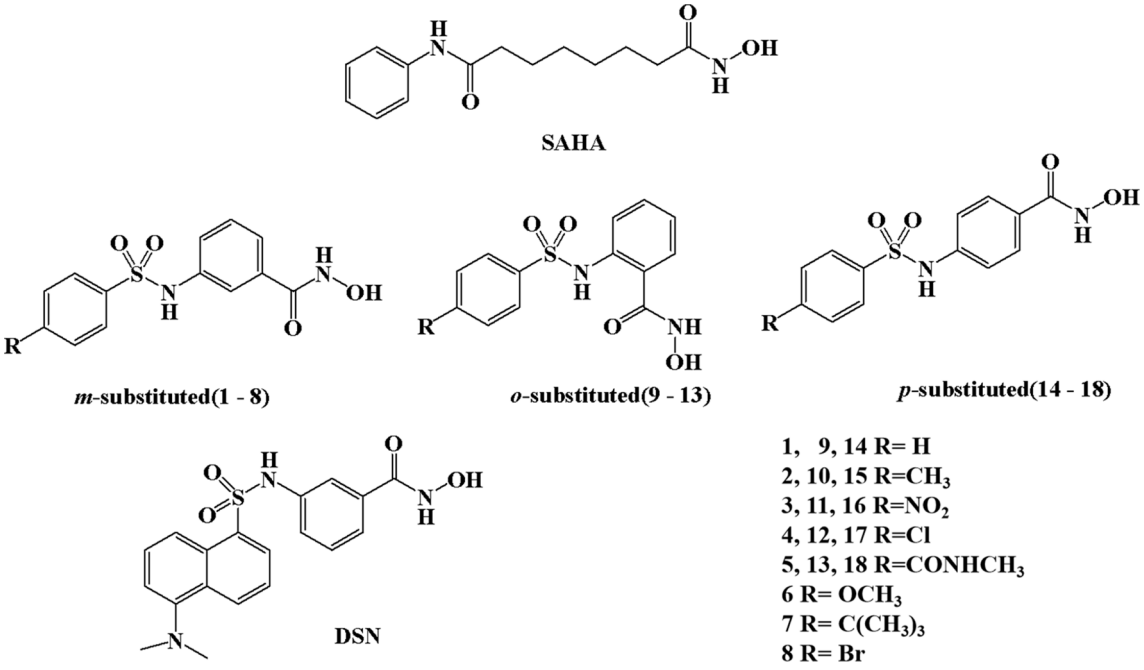

Fig. 1. Structures of the synthesized hydroxamic acids (**1**–**18** and DSN) and the reported hydroxamic acid (SAHA).

Table 1
Inhibitory activity (IC_{50}, μM) of hydroxamic acids against four enzymes as the representatives of MβLs.

Compd.	B1		B2	B3	Compd.	B1		B2	B3
	VIM-2[a]	IMP-1[a]	ImiS[b]	L1[a]		VIM-2[a]	IMP-1[a]	ImiS[b]	L1[a]
m-substituted					*o*-substituted				
1	7.4	7.4	0.9	19.2	**9**	15.4	14.1	0.8	8.3
2	8.4	14.5	0.6	16.3	**10**	17.5	29.9	0.73	19.4
3	5.4	5.2	0.7	13.6	**11**	7.45	19.8	1.2	12.8
4	7.8	7.8	3.2	12.7	**12**	9.4	47.8	4.6	7.8
5	25.4	23.1	7.3	15.1	**13**	43.7	> 50	7.7	13.4
6	21.7	> 50	2.5	27.4	*p*-substituted				
7	11.4	49.7	3.7	6.2	**14**	15.4	19.8	1.0	1.8
8	10.1	12.5	0.9	10.1	**15**	17.2	33.4	0.9	5.2
DSN	16.9	> 50	6.5	9.75	**16**	9.7	32.7	1.6	6.7
SAHA	> 50	> 50	16.7	> 50	**17**	9.9	9.8	5.7	1.3
					18	> 50	> 50	9.4	5.5

[a] The antibiotic used was cefazolin.
[b] The antibiotic used was meropenem.

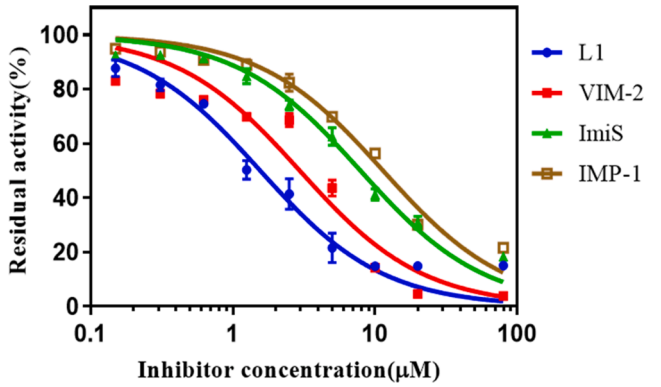

Fig. 2. Inhibition curves of hydroxamic acid **17** against VIM-2, IMP-1, ImiS, and L1.

identify the inhibition mode of the hydroxamic acids against MβLs. Cefazolin as the substrate of L1 for kinetic studies. The concentrations of substrate and the inhibitor were varied between 20–100 μM and 0–80 μM, respectively. After pre-incubation of the enzyme and inhibitor for 3 h, the hydrolysis rates of substrate were determined in triplicate. The inhibition mode was assayed by generating Lineweaver–Burk plots, and K_i values were obtained by fitting initial velocity versus substrate concentration at each inhibitor concentration using SigmaPlot 12.0. The Lineweaver-Burk plots of cefazolin hydrolysis catalyzed by L1 in the absence and presence of hydroxamic acid **17** are shown in Fig. 3. The Lineweaver-Burk plots suggest that the compound is a competitive inhibitor. The K_i value of **17** was determined to be 2.5 μM.

We assayed the time-dependent inhibition of the hydroxamic acid on MβL, and the inhibition curves are shown in Fig. 4. The inhibitory effect of **17** on L1 reached the maximum (>82% inhibition) at a concentration of 10 μM in ~250 min (Fig. 4A), and as the inhibitor concentration increased from 0 to 5 μM, the residual activity of the enzyme decreased (Fig. 4B), implying that the compound displays a slow-binding or slow tight-binding mode.

Considering the effect of Zn(II) concentration on the inhibitory ability of hydroxamic acids with potential metal-chelating motify, inhibition tests of VIM-2 and L1 were performed at three different Zn(II) concentrations (0, 1 and 100 μM). As shown in Fig. 5, the presence of additional free Zn(II) ions has little effect on the IC_{50} value which is in the range of 0.67–1.32 μM for L1 and 5.50–6.90 μM for VIM-2, and inhibitor **17** does not lose its inhibitory ability at a high Zn(II) ions concentration up to 100 μM.

To further study the action mechanism of the hydroxamic acids with MβL, the L1 enzyme was treated with EDTA, 1,4,7-triazacyclononane-*N,N',N''*-triacetic acid (NOTA) and **17** (final concentration is 50 μM), respectively, then dialyzed versus specific buffer. After the dialysate was centrifuged, deionized water was added to make up the solution to the volume before centrifugation and the residual activity of the enzyme was determined. It is clearly observed in Fig. 6 that there is no significant change in enzyme activity before and after treatment with 5% DMSO. When the inhibitors were EDTA and NOTA, the enzyme activity was not restored after treatment. However, it is worth noting that the residual activity of L1 treated by **17** was only 10%, but the activity was restored to 60% after dialysis and centrifugation, indicating that the inhibition of **17** on L1 is reversible.

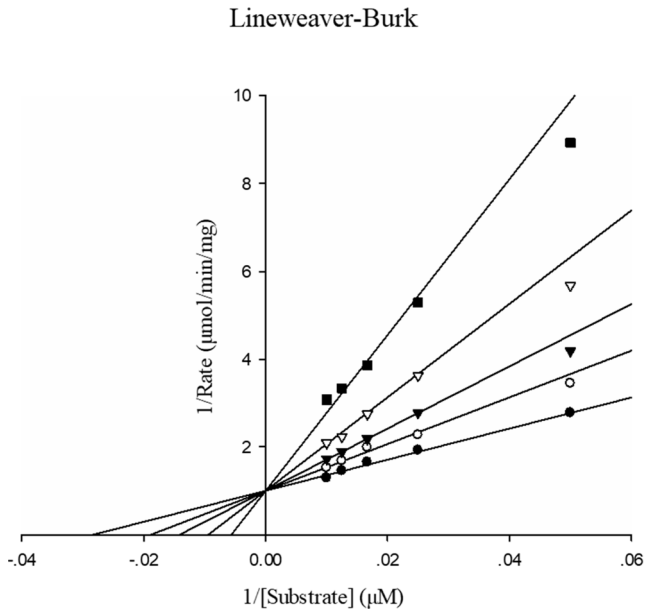

Fig. 3. Lineweaver–Burk plots of L1 catalyzed hydrolysis of cefazolin in the absence and presence of **17**. Inhibitor concentrations were 0 (●), 1.25 (○), 2.5 (▼), 5 (▽), and 10 μM (■).

2.4. Antibacterial activity assays in vitro

To further study the synergistic antibacterial activity of the hydroxamic acids, we determined MICs of antibiotics in the absence and presence of hydroxamic acids (16 μg/mL) as previously reported method [27]. *E. coli*-DH10B cells harboring VIM-2, IMP-1, ImiS, or L1 were used in these assays. The data listed in Table 2A indicated that the hydroxamic acids tested decreased MICs of cefazolin against *E. coli*

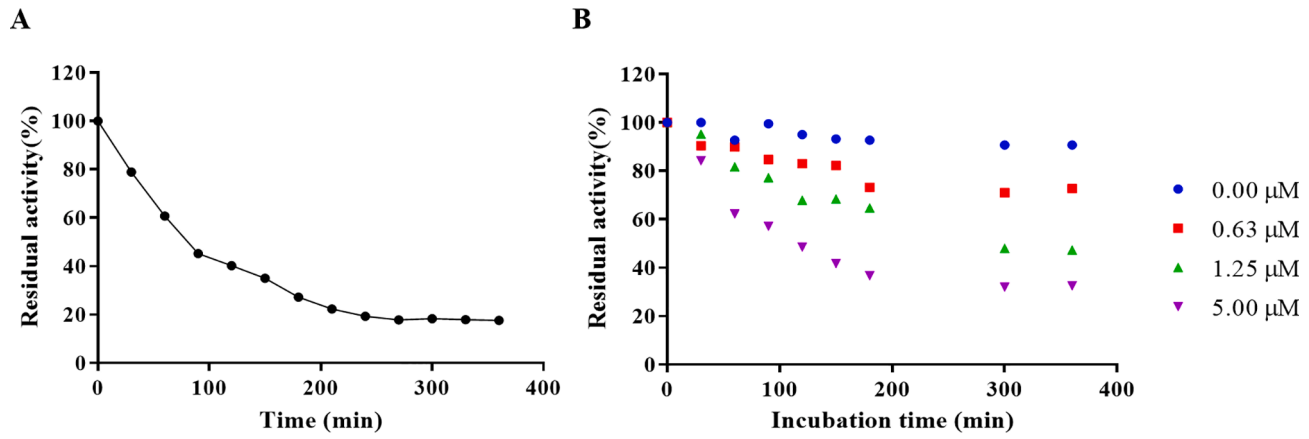

Fig. 4. Time-inhibition curves of L1 by hydroxamic acid **17** at 10 μM (A), and at a concentration between 0.01 and 10 μM (B).

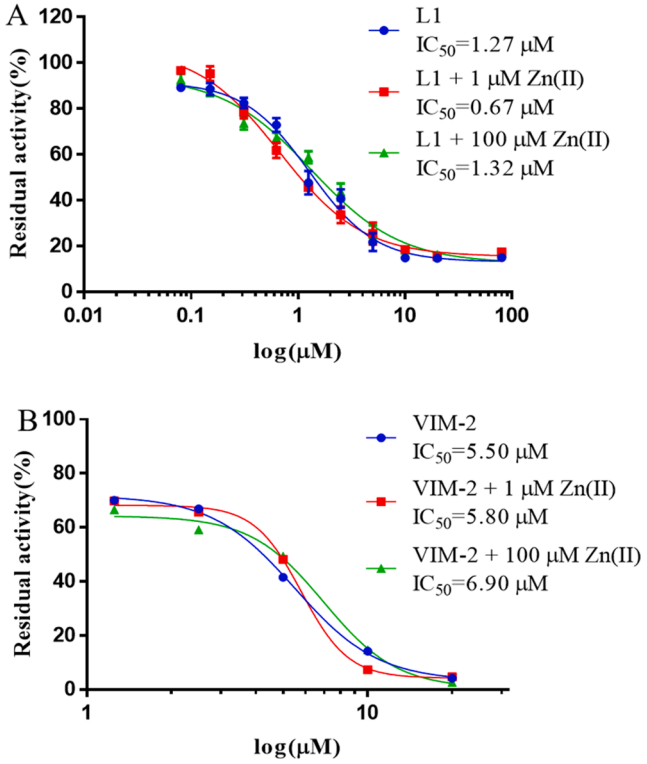

Fig. 5. The dose-inhibition curves of hydroxamic acid **17** on L1 (A) and VIM-2 (B) obtained at three different Zn(II) ion concentrations (0, 1 and 100 μM).

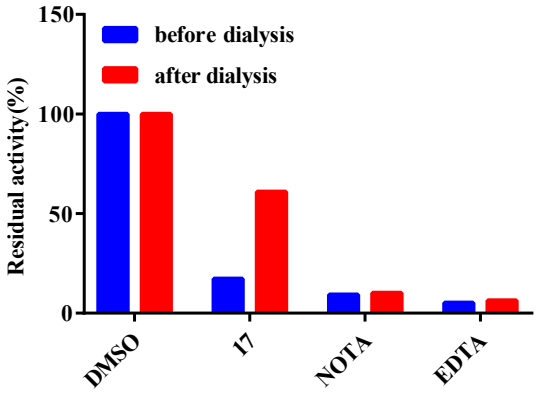

Fig. 6. Residual activity of L1 inhibited by hydroxamic acid **17**, NOTA and EDTA, before and after dialysis and centrifugation. The concentration of inhibitors used was 20 μM.

producing L1, and **17** was found to have the largest effect, resulting in a 32-fold reduction in MIC of the antibiotic. **1**, **3**–**4**, **7**–**9**, **11** and **16**–**17** decreased 2-fold MIC of cefazolin on *E. coli* producing VIM-2 or IMP-1. In addition to **11**–**13** and **16**–**18**, other compounds decreased 2–4-fold MIC of meropenem on *E. coli* with ImiS. Analysis of these MIC data and the corresponding IC_{50} values listed in Table 1 indicates that the inhibitors **7**–**9**, **12** and **14**–**18** and **6** have synergistic antibacterial effect in combination with antibiotics against the *E. coli* with L1 and *E. coli* with ImiS, respectively.

It is worth noting that the *p*-substituted hydroxamic acids significantly increased the antimicrobial effect of cefazolin against *E. coli* expressing L1, resulting in an 8–32-fold reduction in MIC. In view of the excellent broad-spectrum inhibitory effect of *p*-substituted compounds, a dose-dependent MIC assay of **14** and **17** against bacteria expressing L1 was performed. The MIC data listed in Table 2B showed that increasing the dose of inhibitors would lead to a gradual increase in the antibacterial effect of cefazolin. At a dose of 128 μg/mL of **14** and **17**, the MICs of antibiotic were reduced 64 and 128 folds, respectively. In addition, the inhibitor itself does not affect growth of the bacteria, even at a concentration up to 1024 μg/mL.

The antibacterial ability of antibiotics combined with hydroxamic acids was further studied by the inhibition zone experiment. It can be observed in Fig. 7, the combination of cefazolin (CEF) with **14** or **17** resulted in a bigger inhibition area compared to the antibiotic alone, and the inhibitory area of **17** is slightly larger than that of **14**, indicating that **17** had a better effect of restoring antibacterial ability of the antibiotics.

To further probe the action mechanism of hydroxamic acids, metal suppression experiments were performed. Bacterial growth of *E. coli* cells harboring L1 following treatment with NOTA, EDTA or **17** in the presence of Zn(II) ions was assayed. As shown in Fig. 8, when cefazolin (CEF) (36 μM), the inhibitors (240 μM) EDTA, NOTA or **17** were used alone, the bacterial growth rates fluctuated around 95% compared with the negative control. By contrast, when CEF was used in combination with EDTA, NOTA or **17**, the bacterial growth rate decreased sharply. While when Zn(II) ions were pre-cultured with the combination of EDTA or NOTA, the bacterial growth rate rose again and fluctuated around 83%, close to the case that the compounds were used alone. However, the addition of Zn(II) ions basically did not affect the antibacterial activity of CEF in combination with **17**. These data indicate that the growth of bacteria is affected little by the use of these enzyme inhibitors alone, while the combination of these inhibitors with CEF inhibited the growth of bacteria effectively. In addition, the activity of these inhibitors was affected in the presence of additional Zn(II) ions, but did not for hydroxamic acid **17**, implying the different action mechanism.

Table 2
MICs of cefazolin and meropenem combined with hydroxamic acids (16 μg/mL) against *E. coli* Bl21 (EC) producing MβLs (A), and MICs of cefazolin (16 μg/mL) combined with **14** (0–128 μg/mL) or **17** (0–128 μg/mL) against the L1 *E. coli* (B).[a]

A

Inhibitors	EC-VIM-2[b]	EC-IMP-1[b]	EC-ImiS[c]	EC-L1[b]	Inhibitors	EC-VIM-2[b]	EC-IMP-1[b]	EC-ImiS[c]	EC-L1[b]
Blank	128	32	16	32	**11**	64	32	16	16
1	64	16	8	16	**12**	128	32	16	8
2	128	32	8	16	**13**	128	32	16	16
3	64	16	8	16	**14**	128	32	8	2
4	64	16	8	16	**15**	128	32	8	2
5	128	32	8	16	**16**	128	16	16	2
6	128	32	4	16	**17**	64	16	16	1
7	64	32	8	8	**18**	128	32	16	2
8	128	16	8	8	DSN	128	32	16	32
9	128	16	8	4	SAHA	128	32	16	32
10	128	32	8	16					

B

Compd./μg/mL	0	4	16	64	128
14	32	8	2	1	1
17	32	8	1	0.5	0.25

[a] The MICs of cefazolin and imipenem alone against *E. coli* cells without MβLs are 1 and 0.125 μg/mL, respectively.
[b] The antibiotic used was cefazolin.
[c] The antibiotics used was meropenem.

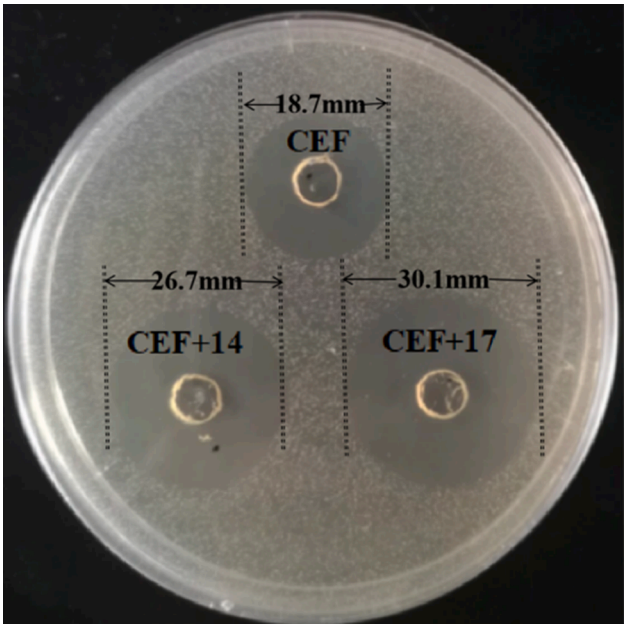

Fig. 7. *E. coli* cells producing L1 were tested by agar disk diffusion assays. CEF: MH with cefazolin only; CEF + **14**: MH with cefazolin and **14**; CEF + **17**: MH with cefazolin and **17**. The concentration of antibiotic and inhibitors used was 32 and 128 μg/mL, respectively.

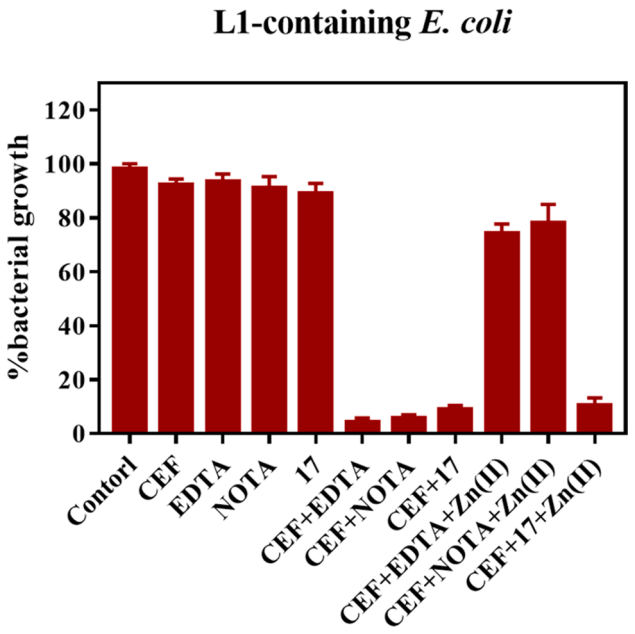

Fig. 8. Growth of *E. coli* cells harboring L1 in the presence of CEF (36 μM, as control), inhibitors (240 μM) EDTA, NOTA or hydroxamic acid **17**, combination of CEF with the inhibitors, and the combination with additional Zn(II) ions. Zn (II) ions were from $ZnCl_2$ (240 μM).

2.5. Cytotoxicity study

In order to determine the cytotoxicity of hydroxamic acids, we selected **1**, **4**, **14** and **17** as representative compounds, and premixed compounds at different concentrations (6.25, 12.5, 25, 50, 100, and 200 μM) with mouse fibroblasts. Fig. 9 shows that even in the case of an inhibitor concentration of up to 200 μM, >80% of the cells tested remained viable, indicating that these hydroxamic acids have low cytotoxicity.

2.6. Antibacterial activity assays in vivo

We selected **17** as a representative compound in combination with cefazolin to treat infected mice to test whether hydroxamic acids can restore cefazolin activity *in vivo* [27]. In short, the systemic infection model of Kunming mice was infected intraperitoneally with a sublethal dose of *E. coli* BL21 cells harboring L1. After infection of the bacteria for 2 h, a single dose of the drug was injected intraperitoneally, and after 24 h of treatment, the effects of combination and monotherapy treatment of **17** and cefazolin on bacterial load in the liver and spleen were examined. The assay results are shown in Fig. 10. It can be observed that the number of colonies treated with the compound alone and the blank control group are not much different, **17** alone had no effect on bacterial burden. But compared with cefazolin monotherapy, co-administration of **17** resulted in a significant reduction of the bacterial load detected in the liver (Fig. 10A) and spleen (Fig. 10B), indicating that the hydroxamic acid **17** had synergistic antibacterial effect *in vivo*.

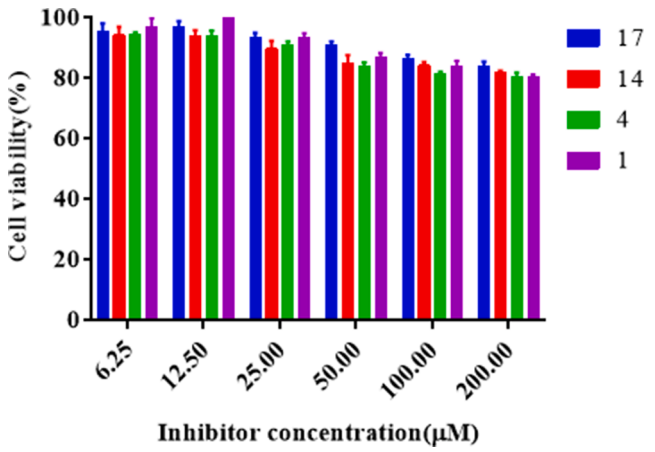

Fig. 9. Percent cell viability (relative to without hydroxamic acid) of L929 mouse fibroblastic cells in the presence of **1**, **4**, **14** and **17** at concentrations of 6.25, 12.5, 25, 50, 100, and 200 μM.

2.7. Docking study

In an effort to explore the binding mode, **17** was selected to dock into the active sites of VIM-2, CphA (in place of ImiS that has not been crystallized yet and shares 96% sequence identity with CphA), and L1 as the representative of B1-B3 subclasses MβLs, and the conformations are shown in Fig. 11. The lowest interaction energy of VIM-2/**17**, CphA/**17**, and L1/**17** complexes was calculated to be −6.95, −8.04, and −7.53 kcal/mol, respectively, indicating that **17** fitted very tightly to the substrate binding site of MβLs.

In the complex VIM-2/**17** (Fig. 11A), one of oxygen atoms of the sulfonamide group is coordinated with two Zn(II) ions (2.2 Å for Zn1 and 1.8 Å for Zn2), and binds to His179 (3.1 Å), while another oxygen atom forms two hydrogen bonds with His179 (3.2 Å) and Asn210 (2.1 Å). Also, one oxygen atom of hydroxamic acid group forms a hydrogen bond with Asn148 (1.9 Å). In complex CphA/**17** (Fig. 11B), one oxygen atom of the sulfonamide group is coordinated with Zn(II) (2.3 Å), and another one binds His196 (1.9 Å) and Asn233 (2.4 Å). In addition, one oxygen atom of the hydroxamic acid group also forms three hydrogen bonds with Phe156 (2.6 Å), Thr157 (3.4 Å) and Gly160 (1.9 Å), respectively. For L1/**17** (Fig. 11C), the hydroxamic acid acted as Zn(II) binding group (ZBG), one oxygen atom of it tightly bound to two Zn(II) (1.9 Å for Zn2 and 1.8 Å for Zn1) and forms two hydrogen bonds with His121 (3.2 Å) and His116 (3.2 Å), while another oxygen atom binds to one Zn(II) (2.5 Å for Zn314) and forms a hydrogen bond with His263 (3.1 Å). These studies reveal that the relatively broad-spectrum activity of compound **17** stems from an ability to utilizes different binding modes to different enzyme, the inhibitor utilizes sulfonamide as ZBG to inhibit VIM-2 and ImiS, but use hydroxamic acid as ZBG to inhibit L1.

The hydroxamic acids **4**, **12** and **17** were selected as the representative of *m*-, *o*- and *p*-substituted derivatives to determine the lowest interaction energy of the complex (enzyme/inhibitor) by molecular docking. As shown in Table S1, the lowest binding energy of complexes of **4**, **12**, and **17** with VIM-2 (-7.77, −7.35, and −6.95 kcal/mol), CphA (-8.29, −8.23, and −8.03 kcal/mol), and L1 (−7.11, −7.24, and −7.53 kcal/mol) is completely consistent with the corresponding IC_{50} values of the inhibitors on three enzymes listed in Table 1. These data support the structure–activity relationship (SAR) gained by enzyme kinetic assays.

3. Conclusions

In summary, nineteen hydroxamic acids with benzenesulfonamides **1**–**18** and DSN were synthesized and characterized by ^{1}H and ^{13}C NMR and HRMS. Biochemical evaluation revealed that hydroxamic acids exhibited broad-spectrum inhibition against four tested MβLs ImiS, L1, VIM-2 and IMP-1 (except **6**, **13** and **18** on IMP-1, and **18** on VIM-2), with an IC_{50} value in the range of 0.6–9.4, 1.3–27.4, 5.4–43.7 and 5.2–49.7 μM, respectively. Analysis of structure–activity relationship revealed that the *m*- and *p*-substituted sulfonyl group improved the inhibitory activity of the hydroxamic acids against VIM-2 and L1, respectively. Compound **17** shows reversible competitive inhibition on L1 with a K_i value of 2.5 μM. The MIC assays indicated that all hydroxamic acids restored antibacterial activity of both cefazolin and meropenem against *E. coli* producing L1, resulting in a 2–32-fold reduction in MIC of the antibiotics. Mice experiments showed that **17** and cefazolin had synergistic antibacterial efficacy in mice infected by *E. coli* producing L1 and significantly reduced the bacterial load in the spleen and liver of mice.

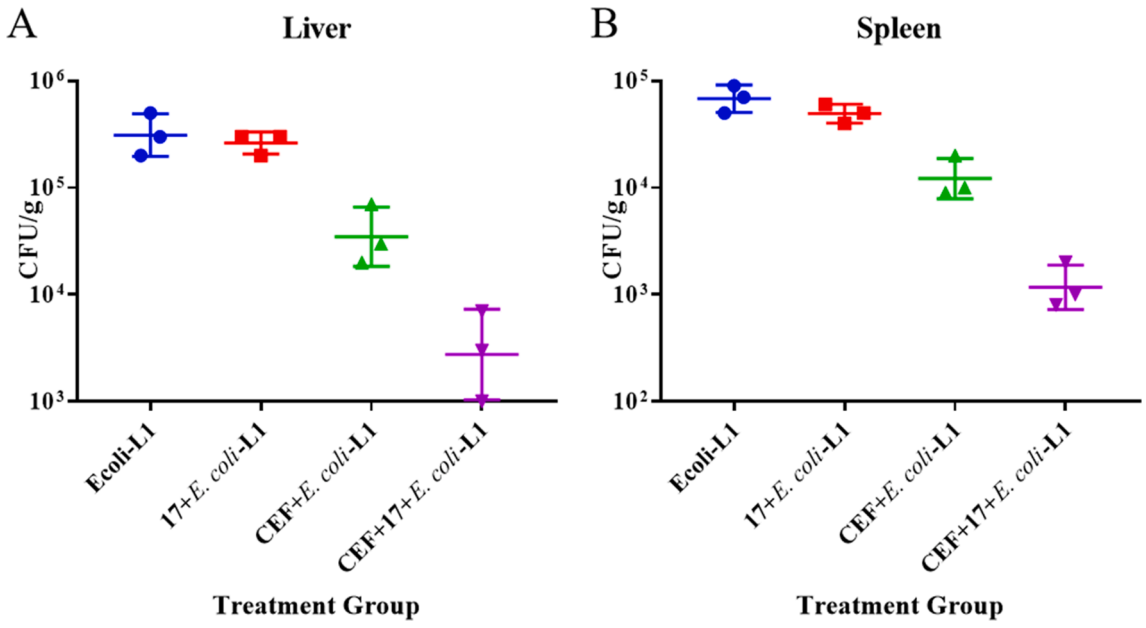

Fig. 10. Hydroxamic acid restores cefazolin activity *in vivo*. Groups of mice infected with L1 *E. coli* BL21 cells were treated with a single dose of cefazolin (10 mg/kg), inhibitor **17** (10 mg/kg), a combination of cefazolin (10 mg/kg) and **17** (10 mg/kg), and *E. coli*-L1 (as control) by intraperitoneal injection. Bacterial load in the spleen (A) and liver (B) was determined by selective plating.

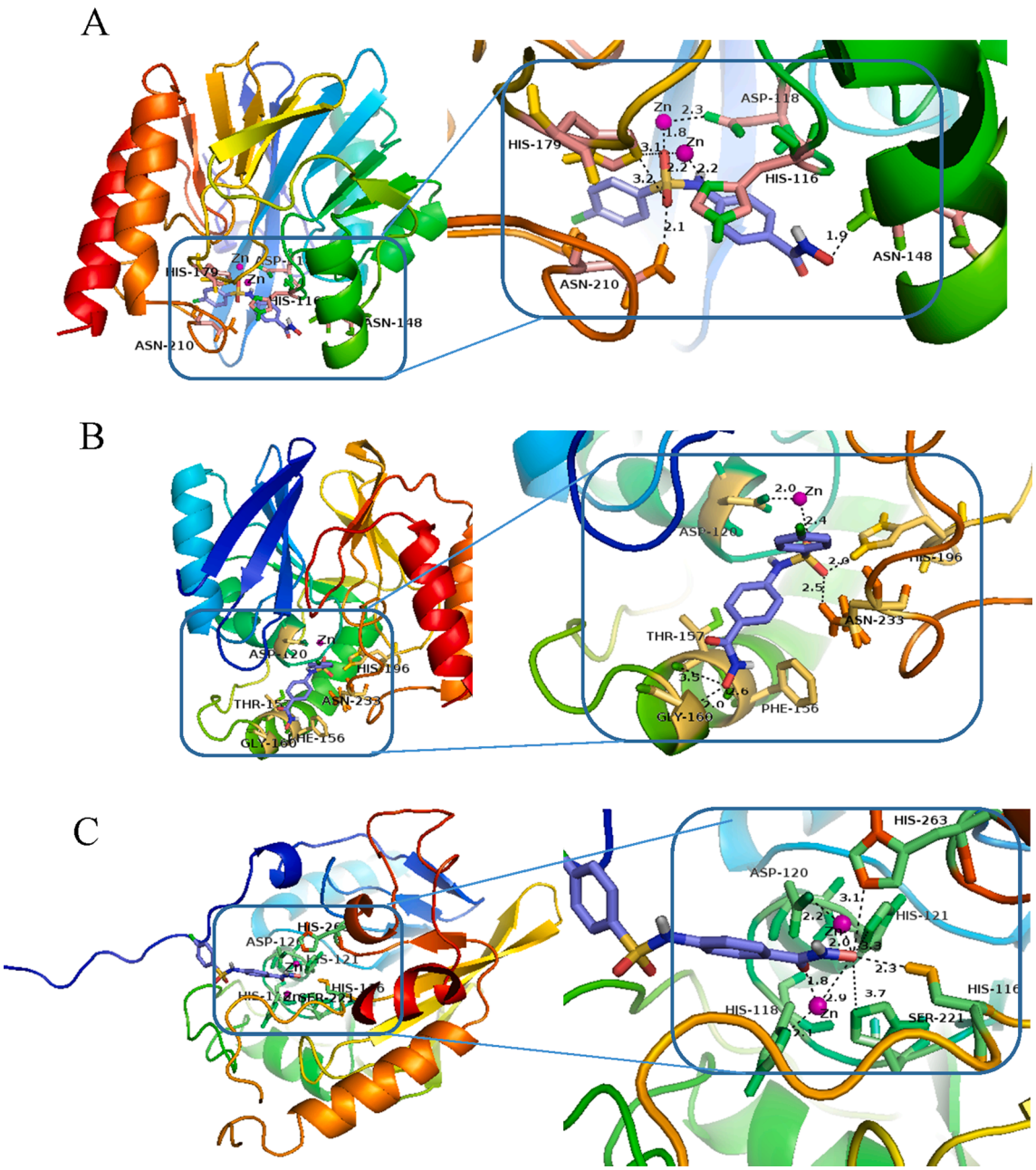

Fig. 11. Lowest-energy molecular docking conformations of **17** docked into the active catalytic site of VIM-2 (11A), CphA (11B) and L1 (11C). The enzyme backbone is shown as a cartoon in rainbow, and hydroxamic acid is shown as sticks colored by element (H, white; C, light-blue; N, blue; O, red; S, yellow; Cl, green). The dotted line indicates the interaction between inhibitor and enzyme residues. All figures were generated with PyMOL. (For interpretation of the references to colour in this figure legend, the reader is referred to the web version of this article.)

The docking studies suggest that the relatively broad-spectrum activity of **17** stems from an ability to utilizes different binding modes to different enzyme, the inhibitor utilizes sulfonamide as ZBG to inhibit VIM-2 and ImiS, but use hydroxamic acid as ZBG to inhibit L1. Cytotoxicity tests showed low toxicity of hydroxamic acids to mouse fibroblasts L929 cells. These studies demonstrate that the hydroxamic acids with benzenesulfonamide are the potent scaffolds for the development of MβLs inhibitors.

4. Experimental

4.1. Materials

Aminobenzoic acids and *N, N*-carbonyldiimidazole were purchased from Shanghai Aladdin Biochemical Technology Co., Ltd. Benzenesulfonyl chlorides were purchased from SAIN Chemical Technology (Shanghai) Co., Ltd-Energy Chemical. Analytical Thin Layer Chromatography (TLC) was performed on silica gel GF254 plates and monitored at an ultraviolet wavelength of 254 nm. ^{1}H and ^{13}C NMR spectra of compounds were determined on a Bruker Avance III 400 MHz NMR spectrometer. Chemical shifts are given in parts per million (ppm) on the delta scale. The peak patterns are reported as singlet (s), doublet (d), triplet (t), quartet (q), doublet (dd), doublet of doublet of doublets (ddd) and multiplet (m). The spectra were recorded with TMS as internal standard. Coupling constants (*J*) were reported in Hertz (Hz). Mass spectra were obtained on a micro TOF-Q (BRUKER) mass spectrometer. Determination of inhibitory activity of compounds on enzyme was performed on Agilent 8453 UV–Vis spectrometer.

4.2. General procedure for preparation of hydroxamic acids (1–18 and DSN) [28,29]

The mixed solution of 3-aminobenzoic acid (1 g, 7.3 mmol) and benzene sulfonyl chloride (1 eq) was slowly added with an aqueous solution of 1 mol/L Na_2CO_3 drop-wise until the solution is clear, reacted at room temperature for 4 h. After the completion of the reaction monitored through TLC, 1 mol/L HCl was slowly added to the mixture and stirred until a large amount of precipitated out and the precipitate was collected [28].

Anhydrous tetrahydrofuran (THF) (5 mL) was added to the mixture of CDI (4.5 mmol, 1.5 eq) and carboxylic acid (3.0 mmol) and was stirred for 1 h. Hydroxylamine hydrochloride (417 mg, 6 mmol) was added and stirred at room temperature overnight (about 16 h). The reaction mixture was diluted with 5% aq. $KHSO_4$ (30 mL) and extracted with EtOAc (2 × 30 mL) and brine (30 mL) and washed. The organic phase was retained and dried with Na_2SO_4 and concentrated in vacuo to give the product [29].

4.2.1. N-hydroxy-3-(phenylsulfonamido)benzamide (1)

Light orange solid, yield 52%. ^{1}H NMR (400 MHz, DMSO) δ 7.72 (d, J = 7.1 Hz, 2H), 7.59–7.45 (m, 4H), 7.32–7.14 (m, 3H). ^{13}C NMR (101 MHz, DMSO) δ 163.85, 139.41, 138.09, 134.03, 133.14, 129.43, 129.31, 126.73, 122.41, 122.14, 119.05. HRMS (ESI) m/z: 315.0401 (Calcd for $[M+Na]^+$ 315.0410 m/z).

4.2.2. N-hydroxy-3-(4-methylphenylsulfonamido)benzamide (2)

Light orange solid, yield 72%. ^{1}H NMR (400 MHz, DMSO) δ 11.16 (s, 1H), 10.39 (s, 1H), 9.02 (s, 1H), 7.64 (d, J = 8.3 Hz, 2H), 7.51 (s, 1H), 7.33 (d, J = 7.9 Hz, 3H), 7.30–7.20 (m, 2H), 2.32 (s, 3H). ^{13}C NMR (101 MHz, DMSO) δ 163.90, 143.52, 138.23, 136.59, 134.03, 129.87, 129.30, 126.80, 122.22, 122.00, 118.87, 21.07. HRMS (ESI) m/z: 329.0544 (Calcd for $[M+Na]^+$ 329.0566 m/z).

4.2.3. N-hydroxy-3-(4-nitrophenylsulfonamido)benzamide (3)

Light orange solid, yield 72%. ^{1}H NMR (400 MHz, DMSO) δ 11.19 (s, 1H), 10.79 (s, 1H), 9.04 (s, 1H), 8.37 (d, J = 9.0 Hz, 2H), 8.00 (d, J = 9.0 Hz, 2H), 7.52 (t, J = 1.8 Hz, 1H), 7.41 (dt, J = 7.7, 1.3 Hz, 1H), 7.32 (t, J = 7.8 Hz, 1H), 7.24 (ddd, J = 8.0, 2.2, 1.1 Hz, 1H). ^{13}C NMR (101 MHz, DMSO) δ 163.68, 150.02, 144.83, 137.37, 134.19, 129.58, 128.38, 124.86, 123.02, 122.84, 119.57. HRMS (ESI) m/z: 360.0244 (Calcd for $[M+Na]^+$ 360.0261 m/z).

4.2.4. 3-(4-chlorophenylsulfonamido)-N-hydroxybenzamide (4)

White solid, yield 55%. ^{1}H NMR (400 MHz, DMSO) δ 11.20 (s, 1H), 10.56 (s, 1H), 9.05 (s, 1H), 7.75 (d, J = 8.5 Hz, 2H), 7.63 (d, J = 8.6 Hz, 2H), 7.52 (s, 1H), 7.39 (d, J = 7.7 Hz, 1H), 7.31 (t, J = 7.8 Hz, 1H), 7.22 (d, J = 7.8 Hz, 1H). ^{13}C NMR (101 MHz, DMSO) δ 163.78, 138.25, 138.06, 137.79, 134.11, 129.64, 129.45, 128.71, 122.75, 122.50, 119.33. HRMS (ESI) m/z: 349.0003 (Calcd for $[M+Na]^+$ 349.0020 m/z).

4.2.5. 3-(4-acetamidophenylsulfonamido)-N-hydroxybenzamide (5)

White solid, yield 65%. ^{1}H NMR (400 MHz, DMSO) δ 11.66 (s, 1H), 10.93 (s, 2H), 9.58 (s, 1H), 8.20 (d, J = 11.7 Hz, 4H), 8.02 (s, 1H), 7.86 (d, J = 7.1 Hz, 1H), 7.79 (t, J = 7.3 Hz, 1H), 7.73 (d, J = 7.5 Hz, 1H), 2.57 (s, 3H). ^{13}C NMR (101 MHz, DMSO) δ 169.20, 163.88, 143.35, 138.33, 133.98, 132.91, 129.25, 128.04, 122.35, 121.96, 119.00, 118.66, 24.24. HRMS (ESI) m/z: 372.0646 (Calcd for $[M+Na]^+$ 372.0625 m/z).

4.2.6. N-hydroxy-3-(4-methoxyphenylsulfonamido)benzamide (6)

White solid, yield 65%. ^{1}H NMR (400 MHz, DMSO) δ 7.71 (d, J = 8.8 Hz, 2H), 7.53 (s, 1H), 7.35 (d, J = 7.5 Hz, 1H), 7.29 (t, J = 7.7 Hz, 1H), 7.23 (d, J = 8.2 Hz, 1H), 7.05 (d, J = 8.9 Hz, 2H), 3.78 (s, 3H). ^{13}C NMR (101 MHz, DMSO) δ 162.61, 138.41, 134.03, 131.09, 129.30, 129.02, 122.19, 121.93, 118.85, 114.56, 55.75. HRMS (ESI) m/z: 345.0514 (Calcd for $[M+Na]^+$ 345.0516 m/z).

4.2.7. 3-(4-tert-butylphenylsulfonamido)-N-hydroxybenzamide (7)

White solid, yield 63%. ^{1}H NMR (400 MHz, DMSO) δ 11.17 (s, 1H), 10.48 (s, 1H), 9.03 (s, 1H), 7.71 (d, J = 8.3 Hz, 2H), 7.57 (d, J = 11.2 Hz, 3H), 7.42–7.19 (m, 3H), 1.25 (s, 9H). ^{13}C NMR (101 MHz, DMSO) δ 163.86, 156.09, 138.29, 136.86, 134.06, 129.33, 126.61, 126.30, 121.83, 118.54, 34.97, 30.81. HRMS (ESI) m/z: 371.1021 (Calcd for $[M+Na]^+$ 371.1036 m/z).

4.2.8. 3-(4-bromophenylsulfonamido)-N-hydroxybenzamide (8)

Light orange solid, yield 72%. ^{1}H NMR (400 MHz, DMSO) δ 7.80–7.59 (m, 4H), 7.53 (s, 1H), 7.39 (d, J = 7.1 Hz, 1H), 7.35–7.09 (m, 2H). ^{13}C NMR (101 MHz, DMSO) δ 163.79, 138.80, 137.96, 134.13, 132.59, 129.48, 128.81, 127.08, 122.78, 122.47, 119.35. HRMS (ESI) m/z: 392.9514 (Calcd for $[M+Na]^+$ 392.9515 m/z).

4.2.9. N-hydroxy-2-(phenylsulfonamido)benzamide (9)

Light orange solid, yield 53%. ^{1}H NMR (400 MHz, DMSO) δ 11.56 (s, 1H), 11.47 (s, 1H), 9.41 (s, 1H), 7.79 (d, J = 7.3 Hz, 2H), 7.63 (t, J = 7.4 Hz, 1H), 7.58–7.51 (m, 3H), 7.51–7.41 (m, 2H), 7.09 (t, J = 8.1 Hz, 1H). ^{13}C NMR (101 MHz, DMSO) δ 165.22, 138.86, 138.13, 133.52, 132.52, 129.58, 127.83, 126.86, 123.60, 119.50, 118.98. HRMS (ESI) m/z: 315.0409 (Calcd for $[M+Na]^+$ 315.0410 m/z).

4.2.10. N-hydroxy-2-(4-methylphenylsulfonamido)benzamide (10)

White solid, yield 57%. ^{1}H NMR (400 MHz, DMSO) δ 11.55 (s, 1H), 11.42 (s, 1H), 9.40 (s, 1H), 7.67 (d, J = 8.1 Hz, 2H), 7.52 (dd, J = 17.4, 7.9 Hz, 2H), 7.43 (t, J = 7.6 Hz, 1H), 7.34 (d, J = 8.0 Hz, 2H), 7.07 (t, J = 7.4 Hz, 1H), 2.32 (s, 3H). ^{13}C NMR (101 MHz, DMSO) δ 165.25, 143.96, 138.28, 136.02, 132.50, 130.00, 127.80, 126.91, 123.40, 119.24, 118.71, 21.08. HRMS (ESI) m/z: 329.0539 (Calcd for $[M+Na]^+$ 329.0566 m/z).

4.2.11. N-hydroxy-2-(4-nitrophenylsulfonamido)benzamide (11)

White solid, yield 54%. ^{1}H NMR (400 MHz, DMSO) δ 11.46 (s, 2H), 9.37 (s, 1H), 8.34 (d, J = 8.5 Hz, 2H), 8.00 (d, J = 8.5 Hz, 2H), 7.50 (dd, J = 13.6, 5.4 Hz, 3H), 7.23–7.10 (m, 1H). ^{13}C NMR (101 MHz, DMSO) δ 164.92, 150.14, 144.19, 136.95, 132.55, 128.55, 128.01, 124.88, 124.63, 120.98, 120.80. HRMS (ESI) m/z: 360.0250 (Calcd for $[M+Na]^+$ 360.0261 m/z).

4.2.12. 2-(4-chlorophenylsulfonamido)-N-hydroxybenzamide (12)

Light orange solid, yield 54%. ^{1}H NMR (400 MHz, DMSO) δ 11.49 (d, J = 48.1 Hz, 2H), 9.41 (s, 1H), 7.77 (d, J = 7.6 Hz, 2H), 7.61 (d, J = 7.6 Hz, 2H), 7.55 (d, J = 7.0 Hz, 1H), 7.47 (s, 2H), 7.12 (s, 1H). ^{13}C NMR (101 MHz, DMSO) δ 164.88, 138.20, 137.49, 132.31, 129.51, 128.62, 127.72, 123.79, 119.91, 119.49. HRMS (ESI) m/z: 349.0002 (Calcd for $[M+Na]^+$ 349.0020 m/z).

4.2.13. 2-(4-acetamidophenylsulfonamido)-N-hydroxybenzamide (13)

White solid, yield 43%. ^{1}H NMR (400 MHz, DMSO) δ 11.44 (d, J = 81.7 Hz, 2H), 10.32 (s, 1H), 9.40 (s, 1H), 7.70 (s, 4H), 7.58–7.39 (m, 3H), 7.07 (s, 1H), 2.05 (s, 3H). ^{13}C NMR (101 MHz, DMSO) δ 169.21, 165.13, 143.59, 138.47, 132.42, 128.96, 128.21, 127.84, 123.29, 119.45, 118.95, 118.73, 24.24. HRMS (ESI) m/z: 372.0645 (Calcd for $[M+Na]^+$ 372.0625 m/z).

4.2.14. N-hydroxy-4-(phenylsulfonamido)benzamide (14)

White solid, yield 73%. ^{1}H NMR (400 MHz, DMSO) 11.07 (s, 1H), 10.71 (s, 1H), 8.99 (s, 1H), 7.84–7.79 (m, 2H), 7.58 (dt, J = 22.8, 7.8 Hz, 5H), 7.15 (d, J = 8.7 Hz, 2H). ^{13}C NMR (101 MHz, DMSO) δ 163.83, 140.52, 139.48, 133.28, 129.54, 128.27, 128.02, 126.80, 118.60. HRMS (ESI) m/z: 315.0413 (Calcd for $[M+Na]^+$ 315.0410 m/z).

4.2.15. N-hydroxy-4-(4-methylphenylsulfonamido)benzamide (15)

White solid, yield 63%. ^{1}H NMR (400 MHz, DMSO) δ 11.04 (s, 1H), 10.59 (s, 1H), 8.94 (s, 1H), 7.68 (d, J = 7.6 Hz, 2H), 7.60 (d, J = 7.5 Hz, 2H), 7.35 (d, J = 7.7 Hz, 2H), 7.13 (d, J = 7.5 Hz, 2H), 2.32 (s, 3H). ^{13}C NMR (101 MHz, DMSO) δ 163.90, 143.72, 140.65, 136.62, 129.97, 128.27, 127.90, 126.89, 118.46, 21.11. HRMS (ESI) *m/z*: 329.0550 (Calcd for $[M+Na]^+$ 329.0566 *m/z*).

4.2.16. N-hydroxy-4-(4-nitrophenylsulfonamido)benzamide (16)

White solid, yield 72%. ^{1}H NMR (400 MHz, DMSO) δ 11.08 (s, 1H), 10.94 (s, 1H), 8.96 (s, 1H), 8.38 (d, J = 8.3 Hz, 2H), 8.04 (d, J = 8.3 Hz, 2H), 7.64 (d, J = 8.2 Hz, 2H), 7.16 (d, J = 8.2 Hz, 2H). ^{13}C NMR (101 MHz, DMSO) δ 163.65, 150.08, 144.77, 139.71, 128.64, 128.41, 124.92, 119.21. HRMS (ESI) *m/z*: 360.0248 (Calcd for $[M+Na]^+$ 360.0261 *m/z*).

4.2.17. 4-(4-chlorophenylsulfonamido)-N-hydroxybenzamide (17)

Light orange solid, yield 74%. ^{1}H NMR (400 MHz, DMSO) δ 11.07 (s, 1H), 10.75 (s, 1H), 8.97 (s, 1H), 7.79 (d, J = 7.6 Hz, 2H), 7.64 (t, J = 7.7 Hz, 4H), 7.14 (d, J = 7.7 Hz, 2H). ^{13}C NMR (101 MHz, DMSO) δ 163.51, 139.90, 138.04, 137.94, 129.48, 128.50, 128.09, 118.67. HRMS (ESI) *m/z*: 348.9999 (Calcd for $[M+Na]^+$ 349.0020 *m/z*).

4.2.18. 4-(4-acetamidophenylsulfonamido)-N-hydroxybenzamide (18)

Light orange solid, yield 44%. ^{1}H NMR (400 MHz, DMSO) δ 10.82 (d, J = 16.0 Hz, 2H), 10.31 (s, 1H), 8.94 (s, 1H), 7.76–7.68 (m, 4H), 7.60 (d, J = 8.7 Hz, 2H), 7.12 (d, J = 8.7 Hz, 2H), 2.05 (s, 3H). ^{13}C NMR (101 MHz, DMSO) δ 169.16, 163.84, 143.39, 140.70, 132.93, 128.16, 127.73, 118.73, 118.42, 24.22. HRMS (ESI) *m/z*: 372.0648 (Calcd for $[M+Na]^+$ 372.0625 *m/z*).

4.2.19. 3-(1-(dimethylamino)naphthalene-5-sulfonamido)-N-hydroxybenzamide (DSN)

Yellow solid, yield 34%. ^{1}H NMR (400 MHz, DMSO) δ 10.92 (s, 1H), 8.43 (d, J = 8.5 Hz, 1H), 8.36 (d, J = 8.6 Hz, 1H), 8.22 (d, J = 7.2 Hz, 1H), 7.67–7.56 (m, 3H), 7.51–7.46 (m, 1H), 7.26 (dd, J = 18.5, 6.2 Hz, 3H), 2.78 (s, 6H). ^{13}C NMR (101 MHz, DMSO) δ 163.82, 151.62, 138.10, 134.53, 133.94, 131.76, 130.45, 129.94, 129.60, 129.08, 128.46, 124.27, 123.65, 122.67, 119.28, 118.57, 115.47, 45.15. HRMS (ESI) *m/z*: 408.0966 (Calcd for $[M+Na]^+$ 408.0988 *m/z*).

4.3. Determination of IC_{50}

VIM-2, IMP-1, ImiS and L1 were over-expressed and purified [30–32], and were selected as representative MβLs for IC_{50} determination. hydroxamic acids **1**–**18** and DSN were dissolved with DMSO to ensure that final concentrations of DMSO is less than 5% during premixing, and MβLs sample and antibiotics were dissolved in 30 mM Tris (pH 7.0). All inhibitors were premixed with the enzyme between 0 and 80 μM and measured, and the antibiotics concentration was 40 μM. The hydrolysis rate of antibiotics was measured on an Agilent UV8453 spectrometer, IC_{50} values were determined by plotting a linear fit of inhibitor concentration and percent inhibition.

4.4. Determination of K_i

At an antibiotic concentration of 20, 40, 60, 80 and 100 μM, the enzyme hydrolysis rates at different inhibitor concentrations were measured and the data were collated using Sigma Plot 12.0 to generate a Lineweaver-Burk plot to determine the hydroxamic acid inhibition mode and K_i value. The hydrolysis rates of antibiotics were obtained by Agilent UV8453 spectrometer.

4.5. Determination of MIC

The minimum inhibitory concentration (MIC) of compounds, antibiotics alone and the combination of antibiotics and inhibitors were determined, respectively, using the broth micro-dilution method. The solutions of *E. coli* containing MβLs (VIM-2, IMP-1, ImiS and L1) were cultivated to OD_{600} = 0.4–0.6, and were diluted 84-fold. Cefazolin was dissolved in MH medium to prepare 4096, 2048, 1024, 512, 256, 128, 64 and 32 (for *E. coli*-VIM-2) and 64, 32, 16, 8, 4, 2, 1 and 0.5 μg/mL (for *E. coli*-IMP-1 and L1), and meropenem was dissolved in MH medium to prepare 64, 32, 16, 8, 4, 2, 1 and 0.5 μg/mL (for *E. coli*-ImiS) stock solutions, respectively. Compounds **1**–**18** and DSN were dissolved in MH solution containing 20% DMSO and diluted to a concentration of 64 μg/mL, 50 μL inhibitor, 50 μL antibiotics with different concentrations and 100uL bacterial solution was mixed and incubated at 37℃ for 16–24 h. Furthermore, **14** and **17** were prepared 512, 256, 128, 64, 32 and 16 μg/mL stock solutions, and was diluted to 200 μL with 50 μL antibiotics solution and 100 μL bacterial solution and incubated for 16–24 h.

4.6. Cytotoxicity assays

A cytotoxicity of inhibitors **1**, **4**, **14** and **17** to mouse fibro-blast cells (L929) was assayed [16]. The cells with a density of 1.0×10^4 cells/well in 100 μL of culture medium were seeded into 96-well plates and maintained for 24 h. Then solutions of inhibitors **1**, **4**, **14** and **17** with work concentrations were added to 96-well plates, respectively, and incubated for another 48 h. Six wells containing only cells suspended in a mixture of 99 μL of complete medium and 1 μL of DMSO were used as the control for investigating cell-viability. Three wells containing only the complete medium were used as the blank control. Following that, the medium was removed, and 100 μL of fresh culture medium and 10 μL of CCK8 were added to each well. After incubation for 4 h, the 96-well plates were then vigorously shaken to solubilize the formed product and the absorbance at a wavelength of 490 nm was read on a Microplate Reader and analyzed. All experiments were conducted in triplicate.

4.7. Metal suppression experiments

In metal suppression experiments, bacterial growth of *E. coli* cells harboring L1 following treatment with NOTA, EDTA or **17** in the presence of Zn(II) ions was assayed. The concentration of CEF was 36 μM, and concentration of Zn(II) ions and inhibitors was 240 μM. *E. coli* cells with OD_{600} of 0.4–0.6 were diluted 84-fold, 3 mL inhibitor (or 3 mL combination of inhibitor and $ZnCl_2$), 3 mL CEF and 6 mL bacteria were mixed and incubated at 37℃ for 16 h. The OD_{600} values of *E. coli* cells were measured on Agilent UV8453 spectrometer. The OD_{600} value of the control group is considered to be 100% bacterial growth rate. The bacterial growth rate of other groups was calculated according to the measured OD_{600} values. The average results were plotted as the mean ± SD of the three experiments.

4.8. Mice experiments

The mice experiment was approved by the Animal Medicine Committee of Xi'an Jiaotong University, and all experimental steps were in compliance with the Guidelines for Care and Use of Laboratory Animals of Xi'an Jiaotong University. Animals were given the sterile ultrapure water and standard commercial diet quantitatively. The mice were randomly divided into four groups, and male and female were cultured separately, with six mice in each group. The bacteria were cultured to an OD_{600} value of 0.8, and 200 μL of bacterial solution was injected into the abdominal cavity of mice. After infection for 2 h, the mice infected group were conducted intraperitoneal treatment with PBS, hydroxamic acid **17**, and cefazolin, a combination of cefazolin and **17**. The injection concentration is 10 mg/kg. The weight of liver and spleen of each mice were kept the same and added with 1 mL of sterile PBS to homogenate for 3–5 min. The slurries were dilute serially, placed 5 μL on LB-agar plates and counted the number of colonies.

Declaration of Competing Interest

The authors declare that they have no known competing financial interests or personal relationships that could have appeared to influence the work reported in this paper.

Acknowledgements

This work was supported by grants from National Natural Science Foundation of China (22077100) and the Shaanxi Province International Cooperation Project (2019KW-068).

Appendix A. Supplementary material

Supplementary data to this article can be found online at https://doi.org/10.1016/j.bioorg.2020.104436.

References

[1] A. Fleming, On the antibacterial action of cultures of a penicillium, with special reference to their use in the isolation of B. influenzae, Clin. Infect. Dis. 2 (1) (1980) 129–139.
[2] X. Ouyang, Y.N. Chang, K.W. Yang, W.M. Wang, J.J. Bai, J.W. Wang, et al., A DNA nanoribbon as a potent inhibitor of metallo-β-lactamases, Chem. Commun. 53 (63) (2017) 8878–8881.
[3] J.F. Fisher, S.O. Meroueh, S. Mobashery, Bacterial resistance to β-Lactam antibiotics: compelling opportunism, compelling opportunity, Chem. Rev. 105 (2) (2005) 395–424.
[4] J. Spencer, T.R. Walsh, A new approach to the inhibition of metallo-beta-lactamases, Angew. Chem., Int. Ed. 45 (7) (2006) 1022–1026.
[5] K. Bush, G.A. Jacoby, Updated functional classification of β-Lactamases, Antimicrob. Agents Chemother. 54 (3) (2010) 969–976.
[6] Z. Hu, G. Periyannan, B. Bennett, M.W. Crowder, Role of the Zn1 and Zn2 sites in metallo-beta-lactamase L1, J. Am. Chem. Soc. 130 (43) (2008) 14207–14216.
[7] G. Garau, I. Garcia-Saez, C. Bebrone, C. Anne, P. Mercuri, M. Galleni, et al., Update of the standard numbering scheme for class B β-Lactamases, Antimicrob. Agents Chemother. 48 (7) (2004) 2347–2349.
[8] C. Bebrone, P. Lassaux, L. Vercheval, J.S. Sohier, A. Jehaes, E. Sauvage, et al., Current challenges in antimicrobial chemotherapy, Drugs. 70 (6) (2010) 651–679.
[9] D.E. Ehmann, H. Jahić, P.L. Ross, R.F. Gu, J. Hu, T.F. Durand-Réville, et al., Kinetics of avibactam inhibition against class A, C, and D β-lactamases, J. Biol. Chem. 288 (39) (2013) 27960–27971.
[10] D.M. Shlaes, New β-lactam–β-lactamase inhibitor combinations in clinical development, Ann. N.Y. Acad. Sci. 1277 (1) (2013) 105–114.
[11] P. Hinchliffe, M.M. González, M.F. Mojica, J.M. González, V. Castillo, C. Saiz, et al., Cross-class metallo-β-lactamase inhibition by bisthiazolidines reveals multiple binding modes, Proc. Natl. Acad. Sci. 113 (26) (2016) E3745–E3754.
[12] S. Skagseth, S. Akhter, M.H. Paulsen, Z. Muhammad, S. Lauksund, Ø. Samuelsen, et al., Metallo-β-lactamase inhibitors by bioisosteric replacement: preparation, activity and binding, Eur. J. Med. Chem. 135 (2017) 159–173.
[13] T. Christopeit, T.J.O. Carlsen, R. Helland, H.K.S. Leiros, Discovery of novel inhibitor scaffolds against the metallo-β-lactamase VIM-2 by SPR based fragment screening, Eur. J. Med. Chem. 58 (21) (2015) 8671–8682.
[14] A.M. King, S.A. Reid-Yu, W. Wang, D.T. King, G. De Pascale, N.C. Strynadka, et al., Aspergillomarasmine A overcomes metallo-β-lactamase antibiotic resistance, Nature 510 (7506) (2014) 503–506.
[15] C. Chen, Y. Xiang, K.W. Yang, Y.Z. Zhang, W.M. Wang, J.P. Su, et al., A protein structure-guided covalent scaffold selectively targets the B1 and B2 subclass metallo-β-lactamases, Chem. Commun. 54 (38) (2018) 4802–4805.
[16] Y. Xiang, C. Chen, W.M. Wang, L.W. Xu, K.W. Yang, P. Oelschlaeger, et al., Rhodanine as a potent scaffold for the development of broad-spectrum metallo-β-lactamase inhibitors, ACS Med. Chem. Lett. 9 (4) (2018) 359–364.
[17] J. Brem, R. Cain, S. Cahill, M.A. McDonough, I.J. Clifton, J.C. Jiménez-Castellanos, et al., Structural basis of metallo-β-lactamase, serine-β-lactamase and penicillin-binding protein inhibition by cyclic boronates, Nat. Commun. 7 (2016) 12406–12414.
[18] R.P. Mcgeary, D.T.C. Tan, C. Selleck, P.M. Monteiro, H.E. Sidjabat, G. Schenk, Structure-activity relationship study and optimisation of 2-aminopyrrole-1-benzyl-4,5-diphenyl-1H-pyrrole-3-carbonitrile as a broad spectrum metallo-β-lactamase inhibitor, Eur. J. Med. Chem. 137 (2017) 351–364.
[19] P. Vella, W.M. Hussein, E.W.W. Leung, D. Clayton, D.L. Ollis, N. Mitić, et al., The identification of new metallo-β-lactamase inhibitor leads from fragment-based screening, Bioorg. Med. Chem. Lett. 21 (11) (2011) 3282–3285.
[20] M.S. Mohamed, W.M. Hussein, R.P. McGeary, P. Vella, G. Schenk, R.H. Abd El-hameed, Synthesis and kinetic testing of new inhibitors for a metallo-β-lactamase from Klebsiella pneumonia and Pseudomonas aeruginosa, Eur. J. Med. Chem. 46 (12) (2011) 6075–6082.
[21] W.M. Hussein, S.S. Fatahala, Z.M. Mohamed, R.P. McGeary, G. Schenk, D.L. Ollis, et al., Synthesis and kinetic testing of tetrahydropyrimidine-2-thione and pyrrole derivatives as inhibitors of the metallo-β-lactamase from Klebsiella pneumonia and Pseudomonas aeruginosa, Chem. Biol. Drug Des. 80 (4) (2012) 500–515.
[22] D.T. Puerta, S.M. Cohen, Elucidating drug-Metalloprotein interactions with tris (pyrazolyl)borate model complexes†, Inorg. Chem. 41 (20) (2002) 5075–5082.
[23] J.L. Roche, P. Bertrand, Inside HDACs with more selective HDAC inhibitors, Eur. J. Med. Chem. 121 (2016) 451–483.
[24] C. Damaskos, S. Valsami, M. Kontos, E. Spartalis, D. Dimitroulis, Histone deacetylase inhibitors: an attractive therapeutic strategy against breast cancer, Anticancer Res. 37 (1) (2017) 35–46.
[25] B.M.R. Liénard, L.E. Horsfall, M. Galleni, J.M. Frère, C.J. Schofield, Inhibitors of the FEZ-1 metallo-β-lactamase, Bioorg. Med. Chem. Lett. 17 (4) (2007) 964–968.
[26] S.K. Kim, M. Demuth, S.R. Schlesinger, S.J. Kim, J. Urbanczyk, R.W. Shaw, et al., Inhibition of Bacillus anthracis metallo-β-lactamase by compounds with hydroxamic acid functionality, J. Enzym. Inhib. Med. Chem. 31 (sup4) (2016) 132–137.
[27] Y. Liu, C. Chen, L.Y. Sun, H. Gao, J.B. Zhen, K.W. Yang, meta-Substituted benzenesulfonamide: a potent scaffold for the development of metallo-β-lactamase ImiS inhibitors, RSC Med. Chem. 11 (2020) 259–267.
[28] X.M. Zha, L.M. Wu, S.Y. Xu, F.X. Zou, J.Y. Xi, T.F. Ma, et al., Design, synthesis and biological activity of N-(3-substituted-phenyl)benzenesulfonamides as selective and reversible LSD1 inhibitors, Med. Chem. Res. 25 (12) (2016) 2822–2831.
[29] N. Usachova, G. Leitis, A. Jirgensons, I. Kalvinsh, Synthesis of hydroxamic acids by activation of carboxylic acids with N, N′-Carbonyldiimidazole: exploring the efficiency of the method, Synthetic Commun. 40 (6) (2010) 927–935.
[30] H. Yang, M. Aitha, A.M. Hetrick, T.K. Richmond, D.L. Tierney, M.W. Crowder, Mechanistic and spectroscopic studies of metallo-β-lactamase NDM-1, Biochemistry 51 (18) (2012) 3839–3847.
[31] M. Aitha, A.R. Marts, A. Bergstrom, A.J. Moller, L. Moritz, L. Turner, et al., Biochemical, mechanistic, and spectroscopic characterization of metallo-β-lactamase VIM-2, Biochemistry 53 (46) (2014) 7321–7331.
[32] P.A. Crawford, N. Sharma, S. Chandrasekar, T. Sigdel, T.R. Walsh, J. Spencer, et al., Over-expression, purification, and characterization of metallo-β-lactamase ImiS from Aeromonas veronii bv. sobria, Protein Expres. Purif. 36 (2) (2004) 272–279.